Characterization of Oxidized Surface Phases on VO_x/ZrO_2 Catalysts

Federica Prinetto and Giovanna Ghiotti*

Dipartimento di Chimica IFM, Università di Torino, Via P. Giuria 7, I-10125 Torino, Italy

Manlio Occhiuzzi and Valerio Indovina

Centro SACSO CNR c/o Dipartimento di Chimica, Università "La Sapienza", Piazzale Aldo Moro 5, I-00185 Roma, Italy

Received: July 24, 1998; In Final Form: September 30, 1998

VO_x/ZrO_2 samples were prepared by three methods: (i) adsorption from aqueous solutions of ammonium metavanadate (AV) at pH 1 or 4; (ii) dry impregnation with AV aqueous solutions at pH 4; and (iii) adsorption from solutions of vanadyl acetylacetonate in toluene. The catalysts were characterized as prepared (a.p.), after evacuation at increasing temperature up to 773 K, after heating in dry oxygen at 773 K (standard oxidation, s.o.), and after reduction in H_2 (or CO), by means of XPS, ESR, and FT-IR spectroscopies. The morphology of pure ZrO_2 and VO_x/ZrO_2 particles was investigated by HRTEM and XRD analysis. Both ZrO_2 and VO_x/ZrO_2 samples with V content $\leq$ 3.5 atoms nm^{-2} showed only zirconia particles with a monoclinic structure. Samples with higher V content contained segregated vanadium phases (V_2O_5 and ZrV_2O_7). On a.p. and s.o. samples with surface V content $\leq$ 3.5 atoms nm^{-2}, XPS showed vanadium species, uniformly spread on the zirconia surface. Depending on the V content, on all reduced samples ESR detected mononuclear V^{IV} in a square pyramidal configuration, and magnetically interacting V^{IV}. On a.p. samples, FT-IR spectra showed the presence of vanadate or metavanadate-type species for V content up to 1.5 atoms nm^{-2} and of decavanadates for V content in the range 1.5−3.5 atoms nm^{-2}. Heating in oxygen at 773 K led to a variety of vanadium species anchored to the zirconia surface: isolated vanadates (prevalent in samples with V content < 0.2 atoms nm^{-2}), low-nuclearity polyvanadates (prevalent in samples with V content up to 1.5 atoms nm^{-2}), and high-nuclearity polyvanadates (prevalent in more concentrated samples, up to 3.5 atoms nm^{-2}). The relative amount of surface species on s.o. samples mainly depended not on the preparation method, but on the vanadium content.

Introduction

Vanadia-based catalysts, mainly supported on TiO_2, Al_2O_3, and SiO_2, have been extensively studied because of their catalytic activity for the selective oxidation of hydrocarbons and their derivatives. A recent issue of *Applied Catalysis* was entirely devoted to this topic.[1] The preparation, characterization, and activity of vanadium oxide monolayer catalysts have been reviewed by Bond and Flamerz Tahir[2] and by Wachs and Weckhuysen.[3]

Previous research has addressed the dispersion, the nuclearity, and oxidation state of vanadium supported systems on TiO_2,[4−13] Al_2O_3,[8,12−22] and SiO_2.[13−15,18,23] Because the dispersion, nuclearity, and oxidation state of vanadium might depend on the support, research also addressed other supports and particularly ZrO_2.[3,24−26] Zirconia is very stable to thermal treatments, has a surface endowed with weak acid and basic sites,[27] and is able to maintain a high specific surface area up to about 1000 K if transition metal ions are present.[28] A recent issue of *Catalysis Today*[29] reviewed the use of ZrO_2 as a support for transition metal oxides.

Vanadium catalysts are also used for environmental catalysis. The commercial catalysts for the selective catalytic reduction of NO with NH_3 in the presence of O_2 (SCR) are $V_2O_5-TiO_2$ and $V_2O_5(-WO_3)/TiO_2$. The SCR process on vanadium-containing catalysts has been extensively reviewed by Bosch and Janssen.[30] Within this framework, we have recently studied the catalytic activity of VO_x/ZrO_2 for the SCR of NO with NH_3. Catalytic results have been reported in full, together with a short summary of the characterization data relevant to the discussion of the catalytic activity.[31] The SCR activity depended only on the V content, not on the method used for catalyst preparation. The marked increase in SCR activity with the V content showed that only specific vanadium configurations were active. This aspect will not be further discussed here. In the present paper we report the HRTEM, XPS, ESR, and FTIR characterization of VO_x/ZrO_2 catalysts prepared by various methods (adsorption from aqueous metavanadate solutions at different pH values, dry impregnation, and adsorption from vanadyl acetylacetonate in toluene). The characterization allowed us to specify the structure of the vanadium polyoxoanions active in the SCR of NO.

Experimental Section

Sample Preparation. The zirconia support was prepared by hydrolysis of zirconium oxychloride with ammonia as previously described;[32] the precipitate was then calcined in air at 823 K for 5 h. After calcination, the BET surface area was SA = 49 $m^2\ g^{-1}$. The VO_x/ZrO_2 catalysts were prepared by three methods: (i) adsorption from aqueous solutions of ammonium

* Author to whom correspondence should be addressed. Phone: +39-011-6707539. Fax: +39-011-6707855. E-mail: ghiotti@ch.unito.it.

10.1021/jp983156i CCC: $15.00 © 1998 American Chemical Society
Published on Web 11/24/1998

metavanadate (AV) (7×10^{-2} to 32 mmol L^{-1}) at pH 1 or 4, fixed by nitric acid; (ii) dry impregnation with AV aqueous solutions at various concentrations and pH 4, fixed by nitric acid; and (iii) adsorption from solutions of vanadyl acetylacetonate, $VO(acac)_2$, in toluene. The specimens were then dried at 383 K for 24 h and ground into a fine powder. The VO_x/ZrO_2 catalysts are designated as ZV*x*(a)pH*y*, ZV*x*(i), or ZV*x*-(acac) where *x* specifies the analytical V content (weight %), where (a), (i), or (acac) indicates the preparation method (i), (ii), and (iii), and *y* is the pH of the AV solution. After dissolving a known amount of the solid in a concentrated (40%) HF solution, the vanadium content was determined by atomic absorption (Varian Spectra AA-30). The *x* range studied was 0.02−4.65 wt %, corresponding to a surface density of 0.045 to 11.9 V atoms nm^{-2}.

NH_4VO_3 was purchased from Carlo Erba (R. P.), $VO(acac)_2$ from Merck-Schuchardt, and V_2O_5 from Aldrich. High-purity gases from Matheson C. P. were used for catalyst treatments without further purification.

The catalysts were studied as prepared (a.p.), after evacuation at increasing temperature up to 773 K, after heating in dry oxygen at 773 K (standard oxidation, s.o.), and after reduction in H_2 or CO. After s.o. treatment, all samples had SA values ranging from 45 to 47 $m^2\ g^{-1}$, slightly smaller than that of pure zirconia.

Characterization Techniques. *XRD and HRTEM Measurements.* The X-ray diffraction analysis of a.p. and s.o. samples was carried out by a Philips PW 1710 diffractometer at 45 kV and 20 mA using the Cu Kα radiation.

Transmission electron microscopies of a.p. and s.o. samples were taken with a JEOL 2000 EX electron microscope equipped with a top entry stage, working at 200 kV. The powders were ultrasonically dispersed in hexane and the suspension was deposited on a copper grid coated with a holey carbon film. The instrumental magnification was 2.5×10^4 to 6×10^5.

XPS Measurements. The XPS spectra were obtained with a Leybold−Hereaus LHS 10 spectrometer (Mg Kα, 1253.6 eV, 12 kV 20 mA) operating in FAT mode and interfaced to a 2113 HP computer. For the analysis, a.p. or s.o. samples were pressed onto a gold-decorated tantalum plate attached to the sample holder. The spectra were collected by computer in a sequential manner: O_{1s}, $V_{2p\ 1/2}$, $V_{2p\ 3/2}$, $Zr_{3d\ 3/2}$, $Zr_{3d\ 5/2}$. BE values were referred to the O_{1s} main peak, taken as 530.0 eV, and were deduced by a best-fitting procedure of the composite peak. More details on spectrum analysis are given elsewhere.[26]

ESR Measurements. The ESR spectra were obtained at RT or 77 K on a Varian E-9 (X band), equipped with an on-line computer for data analysis. Absolute concentration of vanadium species (spins nm^{-2}) were obtained by the ratio between integrated areas of ZV samples and standards, recorded under the same instrumental conditions. As standards, we used vanadium compounds showing ESR spectra with similar hyperfine pattern, line-shape, and line-width: $VO(acac)_2$ (Merck-Schuchardt), $VOSO_5 \cdot 5H_2O$ (Carlo Erba, RP), and vanadyl tetraphenylporphyrin (Midcentury, IL), all in a polycrystalline state.[26]

Before ESR measurement, the specimen was placed in a silica reactor equipped with an ESR silica tube and connected to a circulation apparatus for the thermal treatment. The apparatus was equipped with a magnetically driven pump, a pressure transducer, and a trap placed downstream from the reactor. During all thermal treatments, the trap was kept at 77 K.

FT-IR Measurements. Powdered materials were pelleted in self-supporting disks of 25−35 mg cm^{-2} and 0.1−0.2 mm thickness, placed in an IR cell allowing thermal treatments in vacuo or in controlled atmosphere. All thermal treatments were performed in the presence of a trap at 77 K placed in the vicinity of the activation chamber. After each treatment, FT-IR spectra were run at RT on a Perkin−Elmer 1760-X spectrophotometer equipped with an MCT cryodetector, working in the range of wavenumbers 7200−580 cm^{-1} at a resolution of 2 cm^{-1} (number of scans ∼100).

Data are reported as absorbance spectra or as absorbance difference spectra, as appropriate. For band integration and curve fitting we used the software program "Curvefit, in Spectra Calc" (Galactic Industries Co).

Spectra of reference V_2O_5 and $VO(acac)_2$ compounds in KBr were also recorded.

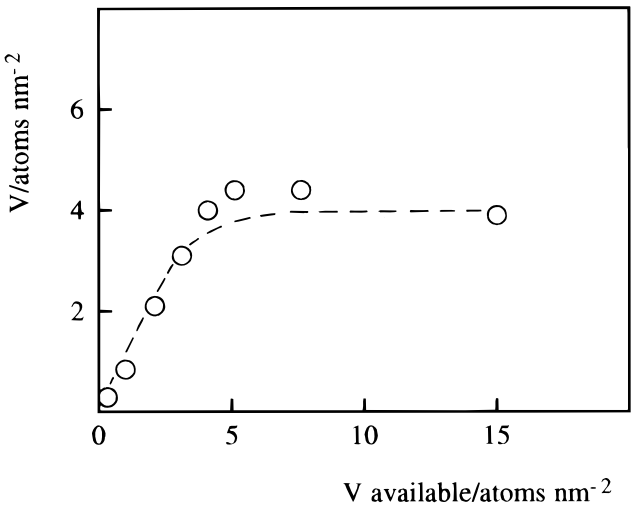

Figure 1. Vanadium uptake on ZrO_2 from vanadyl acetylacetonate solutions in toluene. Vanadium adsorbed (atoms nm^{-2}) as a function of available vanadium in solution (atoms nm^{-2}, referred to the ZrO_2 surface area).

Results and Discussion

Vanadium Uptake. Because the vanadium uptake is a surface phenomenon, we investigated the vanadium adsorbed per unit area of zirconia (atoms nm^{-2}) as a function of V atoms available in the solution used for preparation (atoms nm^{-2} referred to ZrO_2 surface area). From vanadyl acetylacetonate in toluene solution, zirconia adsorbed all vanadium, up to 3.8 atoms nm^{-2}. As the vanadium in solution increased further, uptake reached an extended plateau, corresponding to about 4 V atoms nm^{-2} (Figure 1). Samples prepared by adsorption from AV solutions at pH 2−4 showed an analogous trend, but the maximum uptake was somewhat lower (about 3.5 V atoms nm^{-2}).[26] The difference in the V uptake between ZV(acac) and ZV(a) decreased somewhat after the first evacuation or the first s.o. treatment; the V content in ZV(acac) decreased by about 15%, whereas that in ZV(a) remained unaffected.

Based on the plateau value, ZV samples with V content < 3.5 atoms nm^{-2} will be hereafter referred to as low-loading samples, those with V content > 3.5 atoms nm^{-2} as high-loading samples. We recall that a.p. ZV(a) samples prepared by adsorption from AV solutions with a concentration higher than 10 mmol L^{-1} contain a segregated phase, which transforms into V_2O_5 after the s.o. treatment.[26] Wachs et al., by using Raman spectroscopy, have shown that V_2O_5 up to 6.8 V atoms nm^{-2} is molecularly dispersed on the zirconia surface.[22]

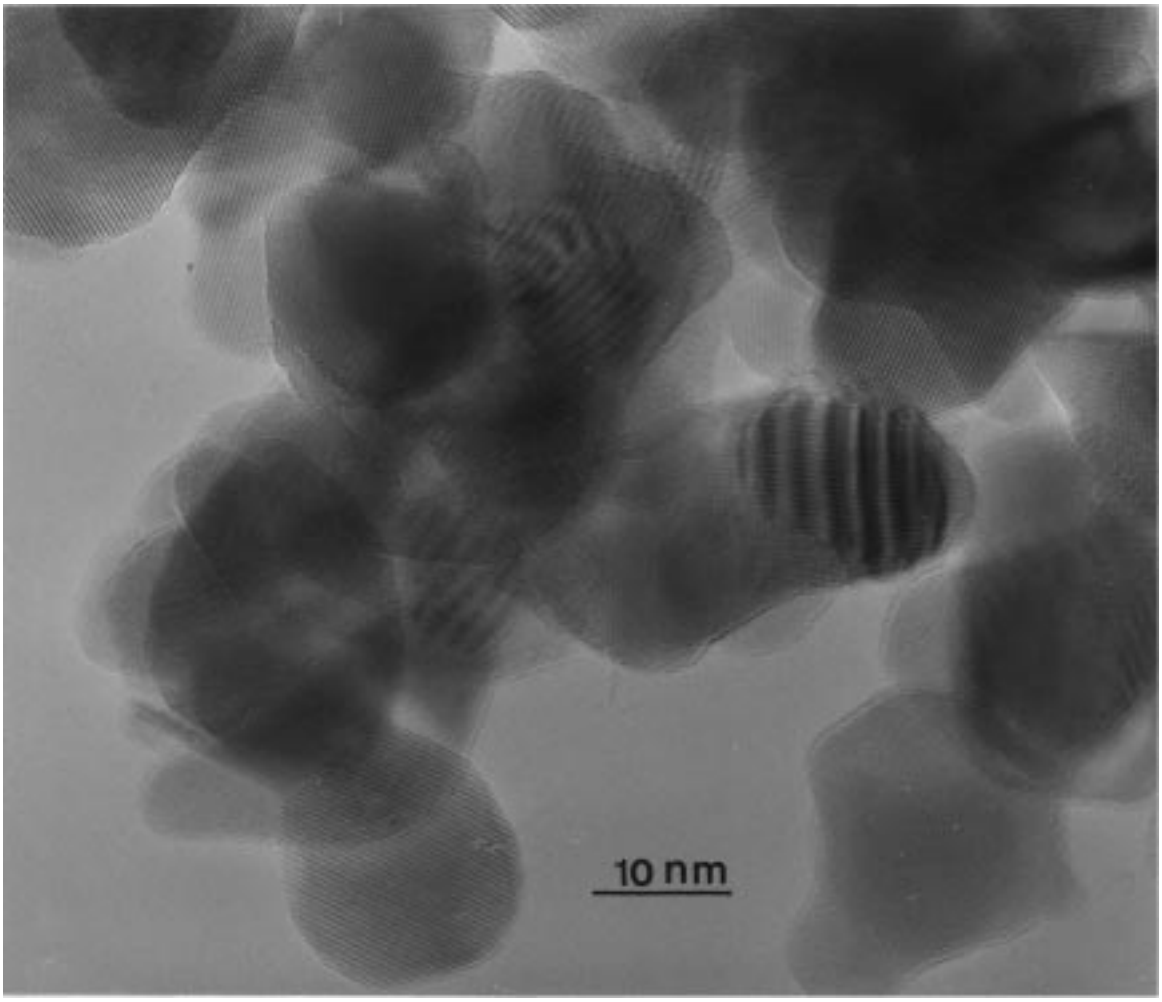

Figure 2. HRTEM image of the as-prepared ZV1.05(i) sample. Instrumental magnification was 6×10^5.

HRTEM and XRD Measurements. Irrespective of the preparation method, pure ZrO_2 and low-loading a.p. and s.o. ZV samples consisted of aggregates of rounded particles with average size 20−30 nm and a monoclinic structure, as revealed by the diffraction-fringes distance, in agreement with the XRD pattern (JCPDS file 36-420). The presence of vanadium left the zirconia morphology unchanged (Figure 2). HRTEM of high-loading a.p. ZV samples showed, in addition to a zirconia phase, 300−600 nm particles having a fibrous shape, possibly arising from polyvanadates or segregated V_2O_5 (Figure 3a). Because these particles were too thick to give electron transmission, HRTEM provided no information on their crystalline structure. In the high-loading s.o. samples, in addition to zirconia particles, two segregated phases were present. One phase, consisting of particles with sharp contours, rectangular shape, and size 300−1000 nm, was the orthorombic V_2O_5 oxide (Figure 3b). For some thinner particles, the distance between the diffraction fringes ($d_{hkl} = 4.28$ and $d_{hkl} = 3.40$ Å) identified the (001) and (110) planes. The assignment relies on the electron micrograph of the reference compound and was confirmed by XRD analysis (JCPDS files 9.387, 41-1426). The second phase, consisting of rare particles with rounded shape and average diameter 100−200 nm, not showing diffraction fringes (Figure 3c), might be attributed to ZrV_2O_7, in agreement with the XRD pattern (JCPDS file 16-422). The ZrV_2O_7 compound formed from the solid-state reaction between ZrO_2 and V_2O_5.[25,33]

XPS Measurements. In s.o. ZV(acac) and a.p and s.o. ZV(i) samples, the binding-energy value of component $V_{2p\,3/2}$, determined by the curve-fitting of the region O_{1s}-V_{2p}, was 517.1 eV, indicating the presence of V^V species only, as already observed in ZV(a) catalysts.[26]

In low-loading ZV(acac) and ZV(i) samples (a.p. and s.o.), the intensity ratios, V_{2p}/Zr_{3d}, increased proportionally to the V content and approached the corresponding values calculated by the spherical model,[34] as already found in the analysis of ZV(a) samples.[31] In high-loading ZV samples, the V_{2p}/Zr_{3d} values were markedly larger than those calculated by the spherical model, pointing to segregation of vanadium phases.

ESR Measurements. In a.p. ZV(acac) samples, a weak ESR signal of V^{IV} species was detected. As in ZV(a) previously studied,[26] no signals were detected in a.p. ZV(i) samples. In all s.o. samples, no signals were detected either after s.o. or after s.o. followed by evacuation at 773 K.

Reduction with CO or H_2 at 573 K of s.o. ZV(acac) and ZV(i) caused the formation of ESR signals. Spectra consisted of a signal showing a resolved hyperfine structure (V_h), overlapping a broad and nearly isotropic band (V_b). In an earlier study we detected the same signals in reduced ZV(a) and assigned them to mononuclear V^{IV} species in a square pyramidal configuration (V_h) arising from the reduction of vanadates, and to magnetically interacting V^{IV} (V_b), arising from the reduction of polyoxoanion units.[26,31] The relative intensities of the two signals depended markedly on the V content (Figure 4, spectra 1−4). In particular, the intensity ratio V_h/V_b (from integrated areas) strongly decreased with increasing V content. We have previously observed very similar dependence of the V_h/V_b ratio on the V content for ZV(a) samples.[26,31]

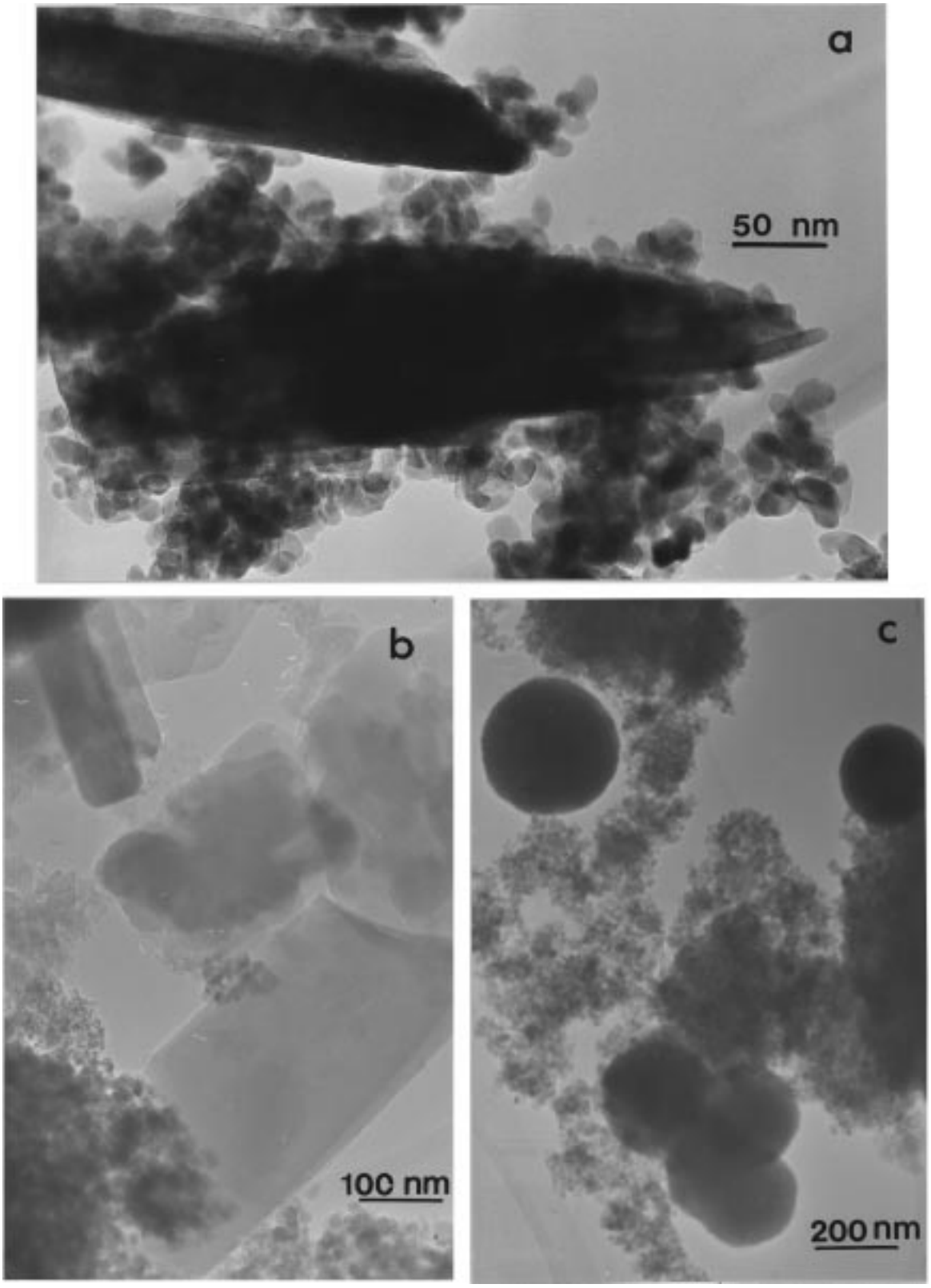

Figure 3. HRTEM images of the as-prepared ZV4.65(a)pH4 sample (a) and after heating in O_2 at 773 K (b and c). Instrumental magnification was 1×10^5 (a), 2.5×10^4 (b), and 5×10^4 (c).

In dilute ZV(acac) and ZV(i) samples (up to 0.2 V atoms nm^{-2}), where isolated V^{IV} (V_h) was the predominant species, the maximum V^{IV} intensity corresponded to 90−60% of total vanadium. In more concentrated samples (0.2 to 3.5 V atoms nm^{-2}), containing therefore increasing amounts of magnetically interacting V^{IV} (V_b), the fraction of total vanadium detected by ESR progressively decreased to 30−15%. In the high-loading samples, ESR detected an even smaller percentage of total vanadium.

Depending on the preparation method, the evacuation at 773 K of a.p. samples gave different results. The evacuation of ZV(a)pH1 and ZV(i) at 773 K gave no ESR signals. Conversely,

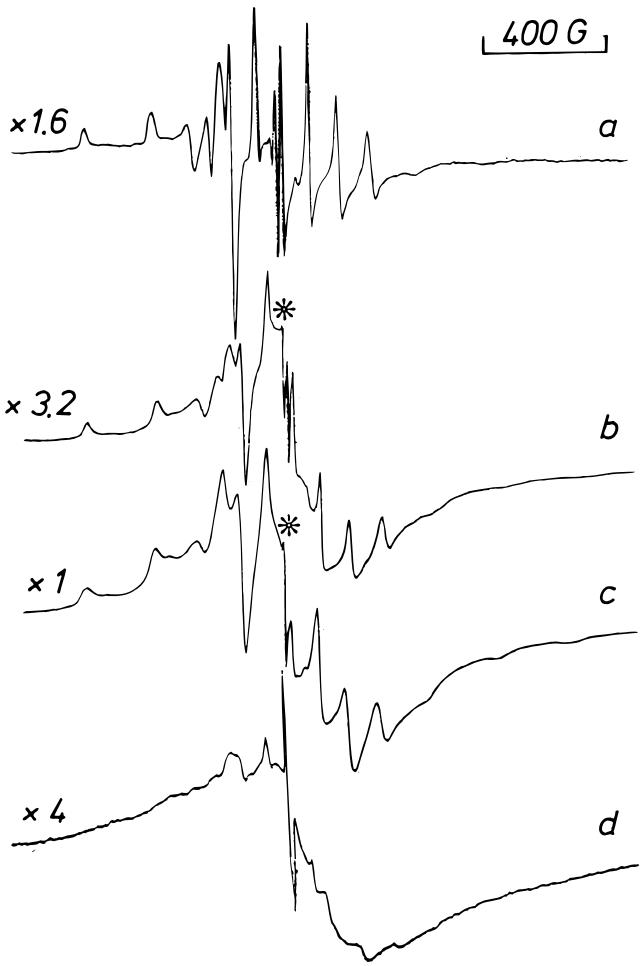

Figure 4. ESR spectra at RT of ZV(acac) samples heated in O_2 at 773 K and reduced thereafter with CO at 573 K. ZV0.14(acac), (curve a); ZV0.30(acac), (curve b); ZV0.58(acac), (curve c); ZV1.20(acac), (curve d). The asterisk indicates the marker at $g = 2.0008$.[26] The figures on each spectrum give the relative gain.

the evacuation of ZV(a)pH4 at the same temperature reduced V^V to V^{IV}, thus yielding ESR spectra similar to those obtained for s.o. samples reduced with CO at 573 K. Irrespective of the preparation method, the evacuation at 773 K of all s.o. samples gave no ESR signal.

FT-IR of Low-Loading Samples. *As-Prepared Samples.* In the 3800−1200 cm^{-1} region (Figure 5), all samples showed a broad absorption at 3760−2600 cm^{-1} and a sharp band at 1620 cm^{-1}, due to surface hydroxyls and coordinated water.

The a.p. samples were distinguished by the following features: (i) in ZV(a)pH4 (curve 1), the presence of carbonates in a very small amount ($\nu_{O=C=O}$ asym mode at 1600−1450, $\nu_{O=C=O}$ sym at 1350−1200, ν_{C-O} at 1060−50 cm^{-1},[35]); (ii) in ZV(a)pH1 (not shown) and ZV(i) (curve 2), the presence of unidentate nitrates ($\nu_{O=N=O}$ asym mode broad band at 1550, $\nu_{O=N=O}$ sym at 1330−1280, ν_{N-O} at 1050−20 cm^{-1} [36]), and ammonium species (δ_{asym} mode at 1460−30 cm^{-1}, δ_{sym} at 1680−60 cm^{-1}, and stretching modes not easily detectable being superposed on hydroxyl and water modes). Ammonium was present in smaller amounts on ZV(a)pH(1) than on ZV(i). In ZV(a)pH1, nitrates were adsorbed from the concentrated HNO_3 solution used to fix the pH of the AV solution, and in ZV(i) the high nitrate concentration was due to the impregnation method that causes all ions to remain on the surface; and (iii) in ZV(acac) (curve 3), the presence of carbonate and acetylacetonate species (broad bands at 1750−1500 and 1450−1250

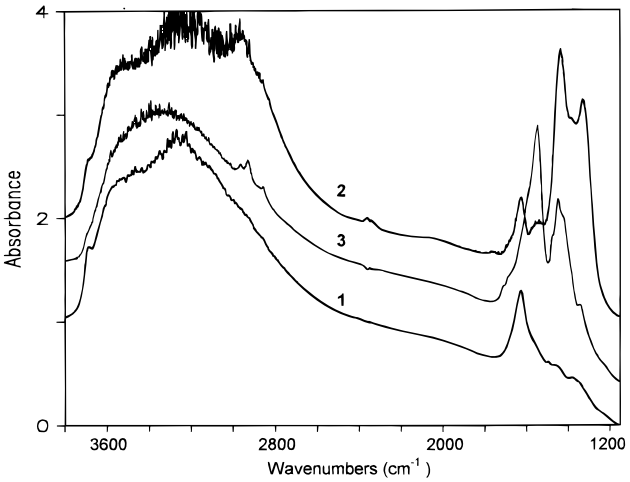

Figure 5. FT-IR spectra of low-loading ZV as-prepared samples in the 3800−1150 cm^{-1} region. ZV0.83(a)pH4, (curve 1); ZV1.05(i), (curve 2); and ZV0.30(acac), (curve 3).

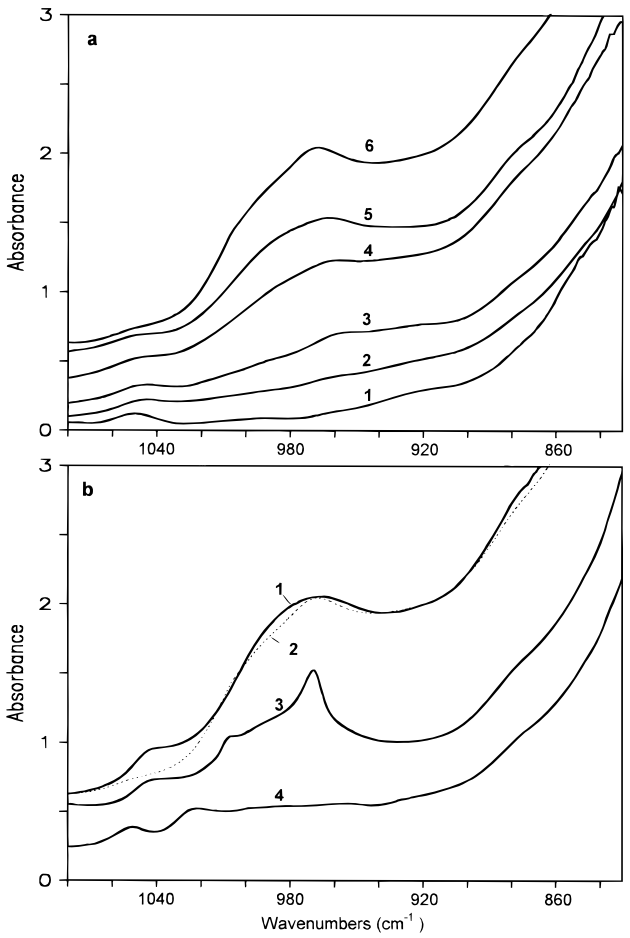

Figure 6. FT-IR spectra of low-loading ZV as-prepared samples in the 1080−830 cm^{-1} region. (a) ZrO_2, (curve 1); ZV0.17(a)pH4, (curve 2); ZV0.34(a)pH4, (curve 3); ZV0.58(a)pH4, (curve 4); ZV0.83(a)pH4, (curve 5); and ZV1.21(a)pH4, (curve 6). (b) ZV1.05(i), (curve 1); ZV1.21(a)pH4, (curve 2); ZV1.03(a)pH1, (curve 3); and ZV0.30(acac), (curve 4).

cm^{-1} [37]), CH_3 and CH_2 groups (bands in the CH stretching region at 3000−2900 cm^{-1}).

In the 1100−830 cm^{-1} region, ZV(a)pH4 samples showed bands at 940−920, 990−960, and 880−850 cm^{-1} (Figure 6a). The intensity of these bands depended markedly on the V content. Notably, the band at 940−920 cm^{-1} was prevalent in samples with V content <1.5 atoms nm^{-2} (curves 2 and 3),

TABLE 1: Most Prominent Raman (R) V−O Bands of Reference Compounds[13,38,39] and IR V−O Bands of ZV As-Prepared Samples in the 1100−830 cm^{-1} Range

species	ν(V=O)[a] (cm^{-1})	ν_{asym} (V−O−V) (cm^{-1})
ref. compd (R)		
$[HV_2O_7]^{3-}$ (at pH 8.5−5.5)	915, 877	
$[(VO_3)_n]^{n-}$ (at pH 8.5−5.5)	945	
$[V_{10}O_{28}]^{6-}$ (at pH 8.5−5.5)	990, 960	840
$[H_nV_{10}O_{28}]^{(6-n)-}$ (at pH 5.5−1.5)	1005, 980	850
cis-$[VO_2F_4]^{3-}$ (at pH < 1.5)	940, 920	
cis-$[VO_2Cl_4]^{3-}$ (at pH < 1.5)	928, 890	
ZV a.p. (IR)		
ZV(a or i)pH4 (<1.5 V atoms nm^{-2})	940−920	
ZV (a or i)pH4 (1.5−3.5 V atoms nm^{-2})	990−960	880−850
ZV(a)pH1 (1.5−3.5 V atoms nm^{-2})	990−960, 1005, 968	
ZV(acac) (0−3.5 V atoms nm^{-2})	1030−980	

[a] Including ν_{sym} and ν_{asym}.

whereas bands at 990−960 and 880−850 cm^{-1} were prevalent in samples with V content 1.5 to 3.5 atoms nm^{-2} (curves 4, 5, and 6). We suggest that the species adsorbed on ZrO_2 are similar to those present in AV solutions with analogous concentrations and pH. Specifically, at pH 4 in dilute AV solution (<10^{-3} M) vanadates, $[H_2VO_4]^-$ are the most abundant species, whereas in concentrated solutions decavanadates, $[HV_{10}O_{28}]^{5-}$ and/or $[H_2V_{10}O_{28}]^{4-}$, are the most abundant species.[13,38] According to the Raman spectra[13,38,39] of the relevant reference compounds (Table 1), we assign (i) the 940−920 cm^{-1} band to the $\nu(V^V{=}O)$ mode of vanadate or metavanadate-type species, (ii) the 990−960 cm^{-1} band to the $\nu(V^V{=}O)$ mode and the 880−850 cm^{-1} band to ν_{asym} (V−O−V) mode of decavanadate-type species.

Spectra of ZV(i) samples closely resembled those of ZV(a)-pH4 with comparable V content (compare curves 1 and 2 in Figure 6b). The main difference was the presence in ZV(i) of a band at 1050−20 cm^{-1}, due to surface nitrates. Spectra of ZV(a)pH1, with V content > 1.5 atoms nm^{-2}, showed the same broad absorption at 990−960 cm^{-1} of ZV(i) and ZV(a)pH4 with similar V content and, in addition, two peaks at 968 and 1005 cm^{-1} (Figure 6b, curve 3). Because at pH 1 in a wide concentration range of AV solutions, VO_2^+ is the most abundant species, we assign the 968 cm^{-1} peak to the ν_{asym} and the 1005 cm^{-1} peak to the ν_{sym} mode of VO_2^+. At pH 1 the ZrO_2 surface is extensively protonated, and therefore anionic species are expected to adsorb. Previous evidence that AV solutions, adjusted to pH 1 with HCl or HF, contain *cis*-$[VO_2Cl_4]^{3-}$ and *cis*-$[VO_2F_4]^{3-}$,[38] suggests that AV solutions adjusted with HNO_3 contain the analogous *cis*-$[VO_2(NO_3)_4]^{3-}$ species (Table 1). The adsorption of *cis*-$[VO_2(NO_3)_4]^{3-}$ -type species on ZrO_2 accounts for the simultaneous presence in ZV(a)pH1 of IR bands from VO_2^+, nitrates, and NH_4^+, the latter species being present as a counterion. Spectra of ZV(acac) showed a broad absorption at 1030−980 cm^{-1} (Figure 6b, curve 4), namely, in the same region as the $\nu(V{=}O)$ bands of pure $VO(acac)_2$ in KBr.

As-Prepared Samples Evacuated at Increasing Temperature. The evacuation of all a.p. samples at increasing temperature caused the complete removal of coordinated water at 423 K and a progressive dehydroxylation. Evacuation up to 773 K caused further dehydroxylation. After this treatment, the amount of free hydroxyls decreased with the V content (Figures 7a and 8a).

The evacuation of ZV(a)pH4 caused a progressive decreasing of carbonates, up to 773 K (Figure 7a). The evacuation at 423 K of ZV(a)pH1 and ZV(i) a.p. transformed unidentate nitrates into bidentate bridged nitrates ($\nu_{N=O}$ at 1600−1500 cm^{-1}, $\nu_{O=N-O}$ asym at 1300−1200 cm^{-1}, and $\nu_{O=N-O}$ sym at 1040−1020 cm^{-1} [31,36]). The evacuation completely removed ammonium species at 523 K and nitrates at 773 K (Figure 8a, a′). The evacuation of ZV(acac) at 773 K removed carbonates and acetylacetonate species (spectra not reported).

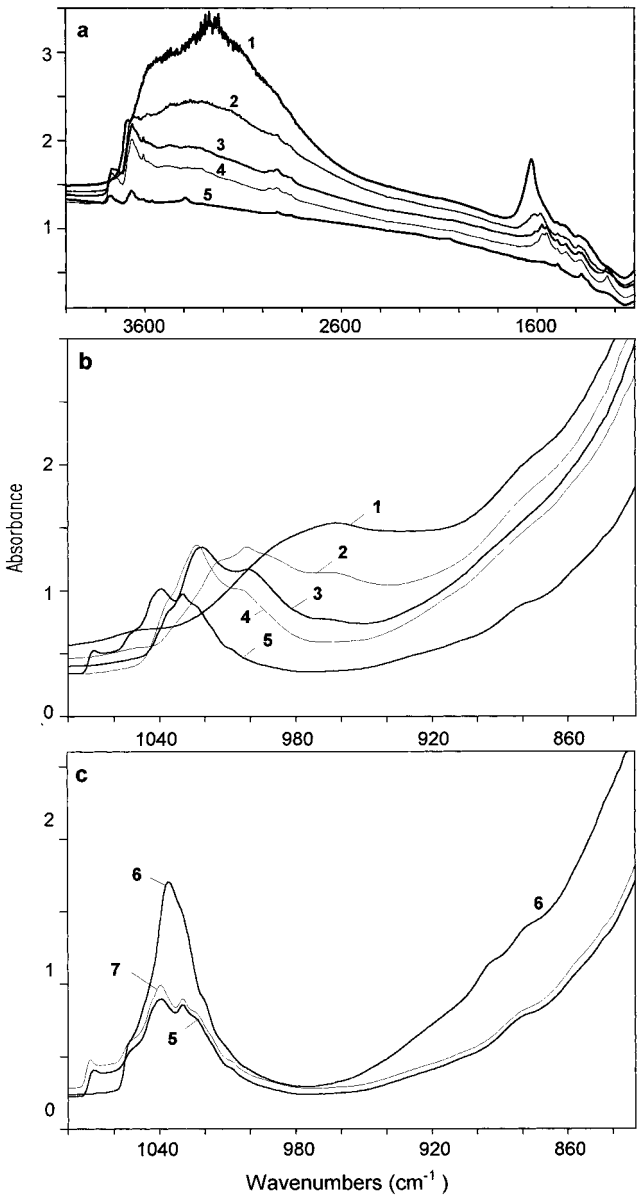

Figure 7. Evacuation at increasing temperature of as-prepared samples prepared by adsorption from NH_4VO_3 solutions at pH 4. FT-IR spectra of ZV0.83(a)pH4 sample in the 3800−1150 cm^{-1} (a), and 1080−830 cm^{-1} regions (b and c). Experiments in sequence: as-prepared sample, (curve 1); evacuated at RT, (curve 2); at 423 K, (curve 3); at 523 K, (curve 4); at 773 K, (curve 5); subsequently heated in O_2 at 773 K, (curve 6); and reduced with H_2 at 773 K, (curve 7).

In the 1100−830 cm^{-1} region, the evacuation of ZV(a)pH4 and ZV(i) at increasing temperature up to 523 K progressively shifted the bands of the different V species toward higher frequency, resolved these bands into several components, and enhanced their intensity (Figure 7b and Figure 8b, curves 1−4). The changes caused by evacuation up to 773 K markedly depended on the sample preparation. This treatment caused the reduction of V^V species in ZV(a)pH4 but not in ZV(a)pH1 and ZV(i) samples. In particular, spectra of ZV(a)pH1 and ZV(i) evacuated at 773 K were nearly coincident with those of s.o.

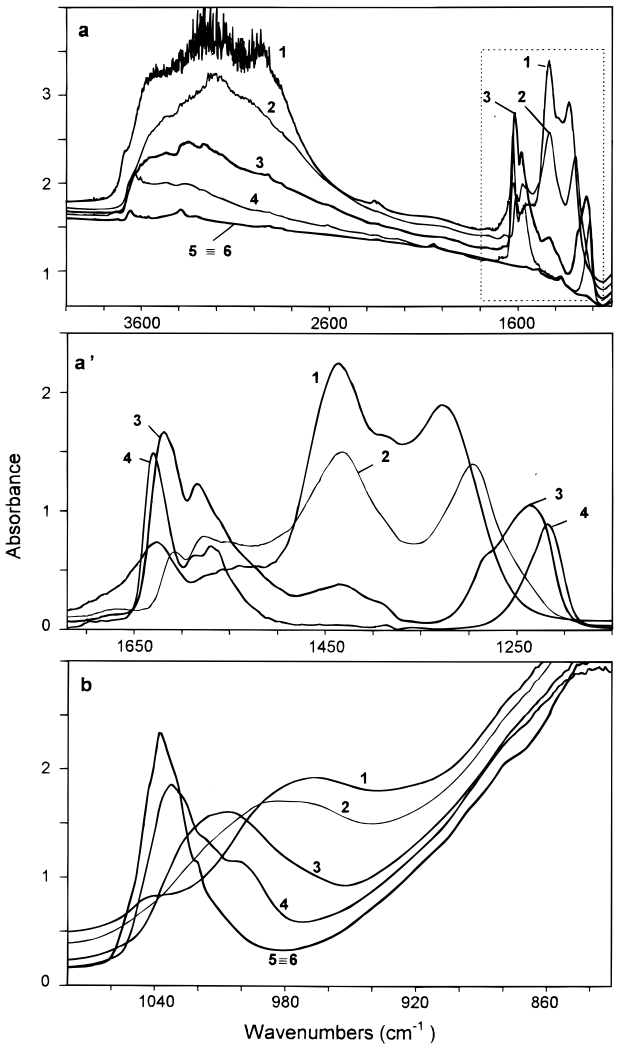

Figure 8. Evacuation at increasing temperature of as-prepared samples prepared by dry impregnation with NH_4VO_3 solutions. FT-IR spectra of ZV1.05(i) sample in the 3800−1150 cm^{-1} (a), 1720−1150 (a′), and 1080−830 cm^{-1} region (b). Experiments in sequence: as-prepared sample, (curve 1); evacuated at RT, (curve 2); at 423 K, (curve 3); at 523 K, (curve 4); at 773 K, (curve 5); heated in O_2 at 773 K, (curve 6).

samples (Figure 8b, curves 5 and 6); whereas spectra of a.p. ZV(a)pH4 and ZV(acac) evacuated at 773 K were nearly identical to those of the corresponding s.o. samples reduced in H_2 at 773 K (compare curves 5 and 7 in Figure 7c).

Samples Heated in O_2 at 773 K. The s.o. treatment of (i) a.p. samples and (ii) a.p. samples previously evacuated at 773 K gave the same IR spectra. After the s.o. treatment, irrespective of the preparation method, with the exception of ZV(a)pH1 with V content < 0.5 atoms nm^{-2}, spectra of ZV samples with the same V content were nearly coincident (Figure 9a,b, curves 3, 3′, 3″ and 6, 6′, 6″).

In the 3800−3000 cm^{-1} region, the amount of free hydroxyls (main bands at 3770 and 3670 cm^{-1} [40,41]) decreased with the V content (Figure 9a). In the region 3000−1100 cm^{-1}, spectra showed only a negligible amount of surface carbonates.

In the 1100−830 cm^{-1} region, spectra consisted of a composite envelope of heavily overlapping bands assigned to the vibrational stretching modes of terminal $V^V{=}O$ groups and to two weak bands at 894 and 874 cm^{-1}. These two bands, nearly absent in all samples with V content < 0.2 atoms nm^{-2} and in ZV(a)pH1 with V content < 0.5 atoms nm^{-2}, are

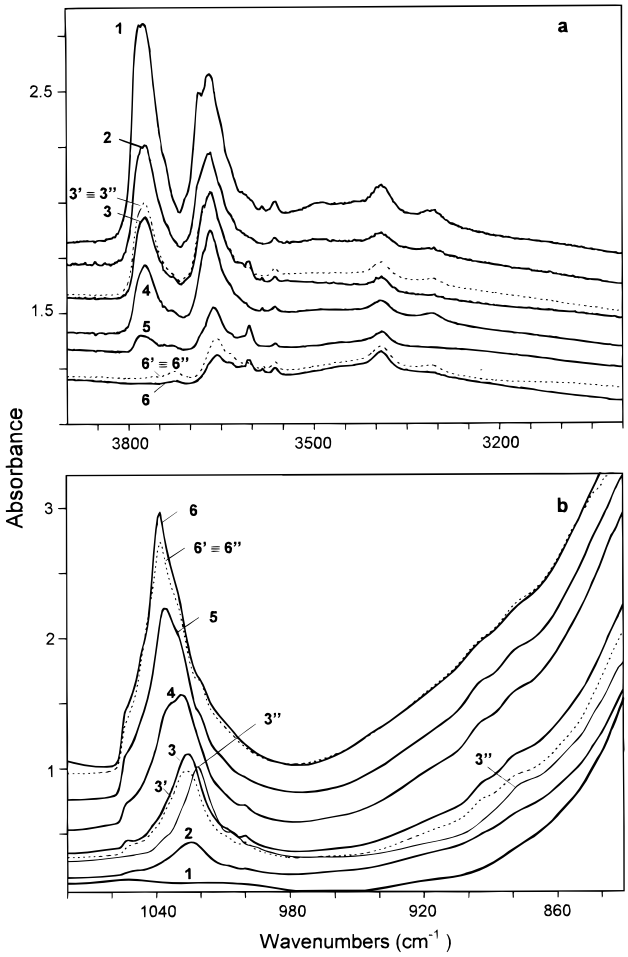

Figure 9. FT-IR spectra of low-loading ZV samples heated in O_2 at 773 K in the 3900−3000 cm^{-1} (a) and 1080−830 cm^{-1} regions (b). ZrO_2, (curve 1); ZV0.17(a)pH4, (curve 2); ZV0.34(a)pH4, (curve 3); ZV0.30(acac), (curve 3′); ZV0.21(a)pH1, (curve 3″); ZV0.58(a)pH4, (curve 4); ZV0.83(a)pH4, (curve 5); ZV1.21(a)pH4, (curve 6); ZV1.05-(i), (curve 6′); ZV1.03(a)pH1, (curve 6″).

tentatively assigned to the ν(V−O−V) modes of polynuclear species (Figure 9b, curves 2 to 6). The absorption edge of the ZrO_2 bulk vibrations shifted upward with increasing V content. A similar effect has been previously observed on MoO_x/ZrO_2 and CrO_x/ZrO_2 systems,[42,43] and attributed to Zr−O−M (M = Mo, Cr, V) stretching vibration modes localized at the surface of zirconia.

In the 1080−980 cm^{-1} region, seven components were identified as peaks and shoulders and analyzed by a curve-fitting procedure (Figure 10a,b). To this aim, the relative intensity of the seven components were left free, the full width at half-maximum (fwhm) were fixed, and a fully Gaussian shape was assumed. The peak position (cm^{-1}) and fwhm (indicated in parentheses, cm^{-1}) were as follows: peak 1, 1001 (5); peak 2, 1009 (9); peak 3, 1019 (9); peak 4, 1026 (9); peak 5, 1037 (10); peak 6, 1043 (10); and peak 7, 1053 (10). Irrespective of the preparation method, the total integrated intensity of the seven peaks increased proportionally to the V content (Figure 10c). The relative intensity of the various components depended not on the preparation method, but on the vanadium content. In particular, in most dilute samples (up to 0.2 atoms nm^{-2}) component 3 predominated, the other components being absent or present at very low intensity. An exception was ZV(a)pH1 samples, in which component 3 predominated up to 0.5 V atoms nm^{-2}. In samples with V loading up to 1.5 atoms nm^{-2}, components 1, 2, and 4 increased together and became prevalent,

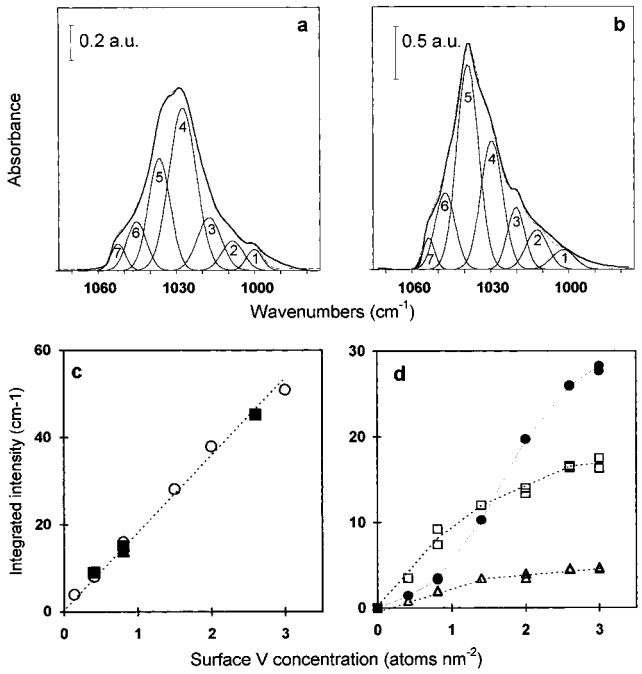

Figure 10. Curve fitting of IR spectra in the 1080−980 cm^{-1} region for low-loading ZV samples heated in O_2 at 773 K: ZV0.58(a)pH4 (a) and ZV1.21(a)pH4 (b). Integrated intensity (cm^{-1}) of the overall absorption in the 1080−980 cm^{-1} region for ZV(a) (○), ZV(i) (■), and ZV(acac) (△) samples as a function of the vanadium content (atoms nm^{-2}) (c). Integrated intensity (cm^{-1}) of type I (△), type II (●) and type III (•) vanadyls as a function of the vanadium content (atoms nm^{-2}) (d).

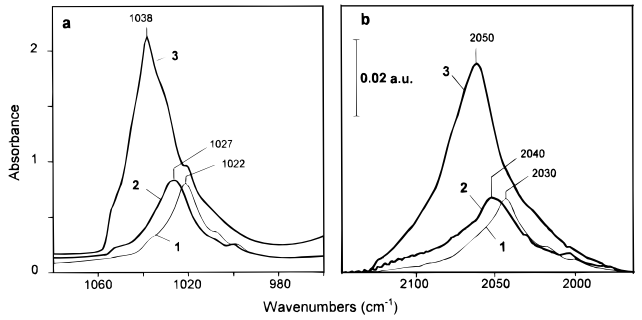

Figure 11. FT-IR spectra of low-loading ZV samples heated in O_2 at 773 K in the ν(V═O) region (a) and in the 2ν(V═O) region (b). ZV0.21(a)pH1, (curve 1); ZV0.34(a)pH4, (curve 2); and ZV1.21(a)-pH4, (curve 3);

whereas component 3 increased little. In more concentrated samples (V content of 1.5 to 3.5 atoms nm^{-2}) components 5, 6, and 7 steeply increased, becoming predominant, whereas all other components remained nearly constant (Figure 10d). On the basis of these intensity changes, we ordered the seven components into three groups: component 3 alone (hereafter referred to as type I vanadyls); components 1, 2, and 4 together (type II vanadyls); and components 5, 6, and 7 together (type III vanadyls).

To obtain further information on the three vanadyl types, we compared the fundamental stretching modes, ν(V═O), with the corresponding first overtones, 2ν(V═O),[44−46] of ZV0.21(a)pH1 (mainly containing type I vanadyls), ZV0.34(a)pH4 (mainly containing type II vanadyls), and ZV1.05(a)pH4 (mainly containing type III vanadyls) (Figure 11). Compared with the fundamental modes, the overtones showed lower intensity (≅ 1/40) and resolution, so that the curve-fitting procedure failed to yield a reliable analysis of these overtones. The 2ν(V═O) overlap, however, resembled strictly that of the corresponding fundamental mode. We therefore suggest that all vanadyls are mono-oxo species, because the spectral features of di-oxo species would have differed, due to the combination of the asym and sym ν(V═O) modes, as reported by Busca et al. for polycrystalline V_2O_5.[44−46] The three selected samples had lower measured overtone maxima values, $2\nu(V{=}O)_{exp}$, than the calculated values, $2\nu(V{=}O)_{calc}$, this pointing to anharmonicity of the V═O oscillators. The value, $\Delta\nu = [2\nu(V{=}O)_{calc} - 2\nu(V{=}O)_{exp}]/2$, can be taken as a measure of V═O oscillator anharmonicity. Type III vanadyls have higher anharmonicity, $\Delta\nu = (2076 - 2050)/2 = 13\ cm^{-1}$, than both type I and type II vanadyls, $\Delta\nu = (2044 - 2030)/2 = (2054 - 2040)/2 = 7\ cm^{-1}$. If the frequency increase observed passing from type I to type III vanadyls were due to an increase of V═O bond strength, we would have found a parallel decrease in anharmonicity, whereas we observed both the highest frequency and anharmonicity for type III vanadyls. Therefore, we suggest that the higher frequency of type III vanadyls results from a dynamic coupling among a large-enough number of nearly parallel vanadyls, belonging to polyvanadate species of high nuclearity and showing a weaker V═O bond than that expected for an isolated vanadyl in a monomeric species. Compared with isolated vanadyls in a monomeric species, vanadyls of polyvanadates are expected to have a weaker double-bond character and therefore a higher anharmonicity. Along the same lines, we propose that type I and type II vanadyls belong to monomeric species or to low-nuclearity polyvanadates.

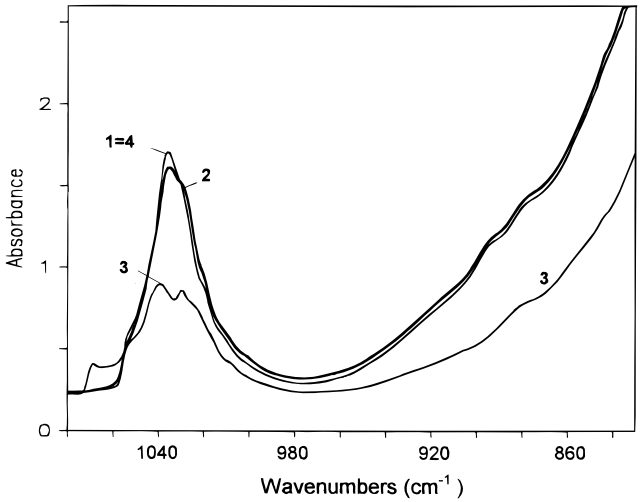

Figure 12. Reversibility of vanadium surface species in redox treatments of low-loading ZV samples. FT-IR spectra of ZV0.83(a)-pH4: sample heated in O_2 at 773 K, (curve 1); evacuated at 773 K, (curve 2); reduced with H_2 at 773 K, (curve 3); heated in O_2 at 773 K, (curve 4).

S.O. Samples Heated at 773 K in Vacuo or in H_2. The evacuation up to 773 K of all s.o. samples caused no changes in the 3800−1100 cm^{-1} and 1100−830 cm^{-1} spectral regions (Figure 12, curves 1 and 2).

Heating in H_2 at 623 or 773 K of all s.o. samples markedly decreased the intensity of the 1100−830 cm^{-1} bands and caused the formation of new components at 1070−1050 cm^{-1}, due to the reduction of V^V (curve 3). A subsequent heating in O_2 completely restored the spectrum of s.o. samples (curve 4). Full reversibility was maintained when the redox cycles were repeated several times.

S.O. Samples Exposed to H_2O. Exposure at RT to water vapor for 30 min of s.o. ZV(a), ZV(i), and ZV(acac) caused the bands in the 1100−830 cm^{-1} region to broaden and shift to a lower

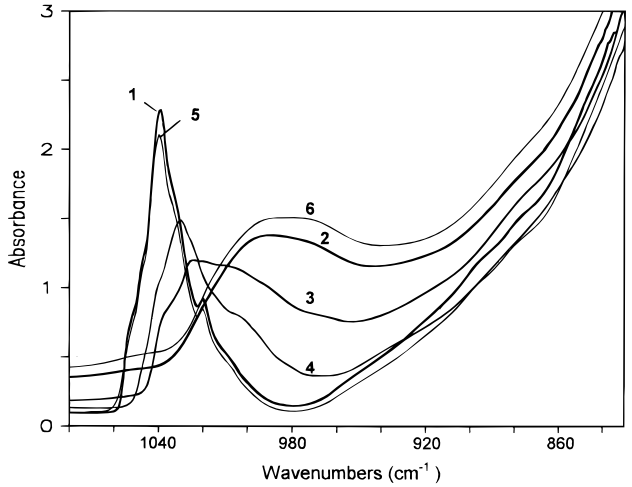

Figure 13. The effect of water vapor addition to low-loading ZV samples previously heated in O_2 at 773 K. FT-IR spectra of ZV1.05(i) after various treatments. Experiments in sequence: sample heated in O_2 at 773 K, (curve 1); contacted with H_2O vapor for 30 min at RT (p_{eq} = 15 Torr), (curve 2); evacuated at RT, (curve 3); at 423 K, (curve 4); at 773 K, (curve 5). The spectrum of the a.p. sample is reported for comparison, (curve 6).

frequency (Figure 13, curves 1 and 2). After this treatment, the spectra of ZV(a) and ZV(i) closely resembled those of the corresponding a.p. sample (compare curves 2 and 6 in Figure 13), whereas spectra of ZV(acac) resembled those of a.p. ZV-(a) and ZV(i) with similar V content. Evacuation up to 773 K of all samples previously exposed to water restored progressively the spectrum of the relevant s.o. sample (Figure 13, curves 3−5). Exposure at RT to water vapor or atmosphere for several weeks and evacuation at 773 K caused the reduction of vanadium, leading to spectra similar to those detected on samples heated in H_2 at 773 K (spectra not reported).

FT-IR of High-Loading Samples. The spectrum of high-loading a.p. samples consisted of two broad and intense absorptions at 1040−980 cm^{-1} and at 950−830 cm^{-1}. The absorption at 1040−980 cm^{-1} consisted of overlapping components at 1026, 1014, and 983 cm^{-1}, that at 950−830 cm^{-1} was superposed on the zirconia bulk vibrations (Figure 14a, curve 1). The spectrum was very similar to that of pure V_2O_5 in KBr, the band at about 1020 cm^{-1} being assigned to $V^V{=}O$ stretching modes and the band at about 820 cm^{-1} to $V^V{=}O$ and V−O−V coupled vibrations.[47]

The evacuation at increasing temperature up to 523 K decreased the absorptions at 950−850 and 1014 cm^{-1} and shifted the 1026 cm^{-1} component toward a higher frequency (Figure 14a, curve 2). Evacuation at 773 K caused a dramatic loss of sample transparency in the whole IR region, a marked intensity decrease of all bands, and the formation of new components at 1069, 1052, 1042, 1033, and 1027 cm^{-1} (curve 3). In addition, new bands at 950, 920, 900, and 878 cm^{-1} became visible. These spectral features are possibly due to the reduction of V_2O_5 to nonstoichiometric VO_x oxides (x = 0.8−1.3),[48] because we observed similar spectra when the s.o. sample was subsequently reduced in H_2 at 773 K (compare curves 3 and 4 in Figure 14a.

The spectrum of high-loading s.o. samples in the 1100−830 cm^{-1} region was similar to that of the corresponding a.p. samples, although the band at 1040−980 cm^{-1} appeared more resolved, showing components at 1040, 1030, 1020, and 983 cm^{-1} (Figure 14b, curve 1). The higher-frequency components most probably arose from supported V species similar to those present in low-loading samples. For high-loading samples the

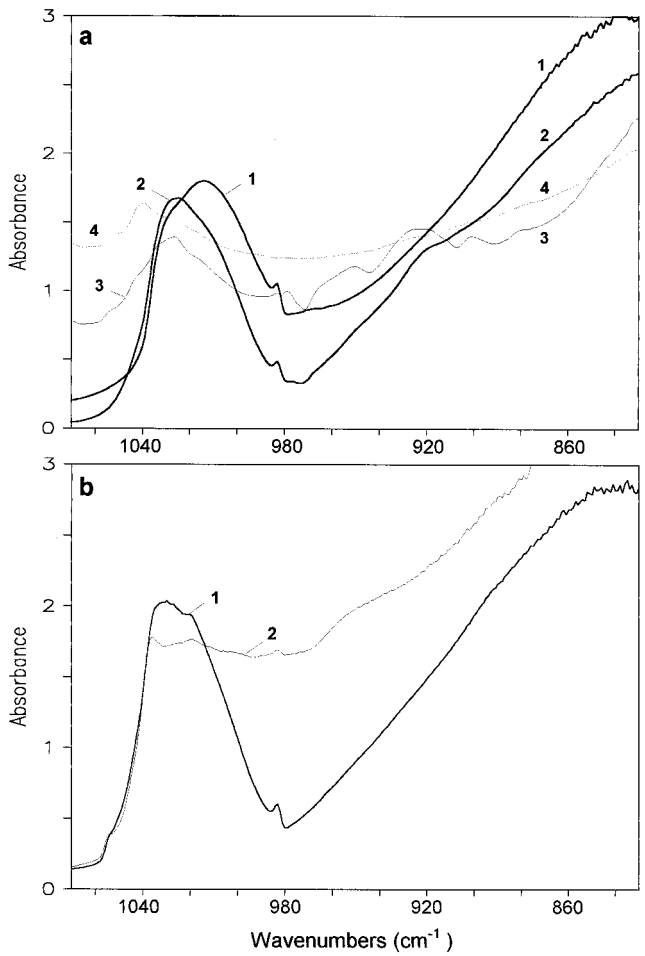

Figure 14. FT-IR spectra of high-loading ZV samples in the 1080−830 cm^{-1} region. ZV4.65(a)pH4 after various treatments. (a) Experiments in sequence: as-prepared sample, (curve 1); evacuated at 523 K, (curve 2); at 773 K, (curve 3); heated in O_2 at 773 K and reduced with H_2 at 773 K, (curve 4). (b) Sample heated in O_2 at 773 K, (curve 1); heated in O_2 at 773 K after 3−4 redox cycles, (curve 2).

overlapping of these components with strong bands from segregated V_2O_5 did not allow reliable curve-fitting analysis.

The spectrum of s.o. samples obtained after 3−4 redox cycles markedly differed from that observed after the first s.o. treatment. After several redox cycles, we observed a marked increase of a broad absorption at 1040−830 cm^{-1}, possibly due to the formation of a new massive phase (Figure 14b, curve 2).

The Anchorage Process of Vanadium Species. Having reported above the spectroscopic features and the assignment of IR, ESR, and XPS spectra, in the following we will focus on the surface chemistry processes taking place during the heating of ZV samples under vacuum and in oxygen at 773 K.

In low-loading a.p. samples, in addition to the vanadium species (hydrated vanadates, decavanadates, and vanadyls), carbonates, nitrates, acetylacetonates, and ammonium are present, depending on the preparation method.

In low-loading samples heated in O_2 at 773 K, irrespective of the preparation method and preceding treatments, carbonates, nitrates, acetylacetonates, and ammonium are absent. In these samples, XPS shows the presence of V^V species only, uniformly spread on the zirconia surface. Overall, ESR and IR results identify three vanadium species: (i) isolated vanadates prevalent in samples with V content < 0.2 atoms nm^{-2}; (ii) low-nuclearity polyvanadates, prevalent in samples with V content up to 1.5 atoms nm^{-2}; and (iii) high-nuclearity polyvanadates, prevalent in more concentrated samples, up to 3.5 atoms nm^{-2}. The

relative amount of vanadates and polyvanadates depends only on the V content and not on the preparation method, with the noticeable exception of ZV(a)pH1 samples, on which, in the concentration range 0.2−0.5 V atoms nm^{-2}, the amount of monomers is much higher than that observed in the corresponding ZV(a)pH4, ZV(i), and ZV(acac) samples, as discussed above.

The vanadium anchorage to the zirconia surface takes place through water elimination between adsorbed vanadium species and the hydroxo groups of the zirconia surface, leading to ($-O_mV_n-O-Zr-$) species. In agreement, irrespective of the preparation method, we detected a decreasing amount of hydroxyl groups in s.o. ZV samples with increasing V content.

After evacuation at increasing temperature up to 773 K of a.p. ZV(a)pH4, IR and ESR showed the reduction of vanadates and polyvanadates to species containing V^{IV}. The evacuation of ZV(i) and ZV(a)pH1 at increasing temperature did not reduce vanadates and polyvanadates, most probably because NO and NO_2 evolving from the nitrate decomposition prevent reduction.

For all samples, once anchored to the zirconia surface, vanadates and polyvanadates are neither reduced upon evacuation at 773 K nor upon exposure for 30 min to H_2O followed by evacuation at 773 K. The heating with CO or H_2 at 573−773 K reduced V^V to V^{IV}. The subsequent heating with O_2 at 773 K reversibly restored surface vanadates and polyvanadates.

The exposure of all s.o. samples to the atmosphere or water vapor for several weeks, dis-anchored vanadates and polyvanadates from the surface. For all ZV samples, after dis-anchorage, evacuation at 773 K reduced vanadates and polyvanadates.

The XPS of a.p. and s.o. high-loading ZV samples showed poor spreading of vanadium species on ZrO_2. The XRD, HRTEM, and FT-IR of the s.o. high-loading samples showed segregated V_2O_5 and ZrV_2O_7, the latter irreversibly formed through the solid-state reaction between ZrO_2 and V_2O_5.

Conclusions

The heating in O_2 at 773 K of VO_x/ZrO_2 with V content up to 3.5 atoms nm^{-2} stabilizes surface vanadates of various nuclearities, uniformly spread on the ZrO_2 support. For sample with a V content up to 1.5 atoms nm^{-2}, monomeric and low-nuclearity V species prevail, whereas in the concentration range 1.5−3.5 atoms nm^{-2} higher-nuclearity V species, possibly decavanadates, prevail. Samples with V content > 3.5 atoms nm^{-2} contain V_2O_5 and ZrV_2O_7. The relative abundance of the various V species mainly depends on the V content, not on the method used for catalyst preparation. This finding strengthens that the nuclearity of the adsorbed species is mostly controlled by the acid−base properties of the support.[42,49]

The marked increase in the SCR activity of VO_x/ZrO_2 with the vanadium content[31] is due to the increased concentration of polynuclear vanadium species.

Acknowledgment. Financial support was provided by the Ministero dell'Università e della Ricerca Scientifica e Tecnologica (Progetti di rilevante interesse nazionale).

References and Notes

(1) Vanadia catalysts for selective oxidation of hydrocarbons and their derivative. Grybowska-Swierkosz, B., Trifirò, F., Vedrine, J. C., Eds.; *Appl. Catal., A* **1997**, *157*.
(2) Bond, G. C.; Flamerz Tahir, S. *Appl. Catal.* **1991**, *71*, 1.
(3) Wachs, I. E.; Weckhuysen, B. M. *Appl. Catal., A* **1997**, *157*, 67.
(4) Rusiecka, M.; Grzybowska, B., Gasior, M. *Appl. Catal.* **1984**, *10*, 101.
(5) Centi, G.; Giamello, E.; Pinelli, D.; Trifirò, F. *J. Catal.* **1991**, *130*, 220.
(6) Soria, J.; Conesa, J. C.; Lopez Granados, M.; Mariscal, R.; Fierro, J. L. G.; Garcia de la Banda, J. F.; Heinemann. H. *J. Catal.* **1989**, *120*, 457.
(7) Odriozola, J. A.; Soria, J.; Somorjai, G. A.; Heinemann, H.; Garcia de la Banda, J. F.; Lopez Granados, M.; Conesa, J. C. *J. Phys. Chem.* **1991**, *95*, 240.
(8) Gil-Llambìas, F. J.; Escudey, A. M.; Fierro, J. L. G.; Lopez Agudo, A. *J. Catal.* **1985**, *95*, 520.
(9) Lars S.; Andersson, T. *J. Chem. Soc., Faraday Trans. 1* **1979**, *6*, 1356.
(10) Kantcheva, M. M.; Bushev, V.; Klissurski, D. *J. Catal.* **1994**, *145*, 96.
(11) Ciambelli, P.; Lisi, L.; Russo, G.; Volta, J. C. *Appl. Catal., B Environmental* **1995**, *7*, 1.
(12) Eckert, H.; Wachs, I. E. *J. Phys. Chem.* **1989**, *93*, 6796.
(13) Deo, G.; Wachs, I. E. *J. Phys. Chem.* **1991**, *95*, 5889.
(14) Van Rejen, L. L. Cossee, P. *Discuss. Faraday Soc.* **1966**, *41*, 277.
(15) Shvets, V. A.; Kazansky, V. B. *J. Catal.* **1972**, *25*, 123.
(16) Inomata, M.; Mori, K.; Miyamoto, A.; Murakami, Y. *J. Phys. Chem.* **1983**, *87*, 761.
(17) Jonson, B.; Rebenstorf, B.; Larsson R.; Lars, S.; Andersson, T.; Lundin, S. T. *J. Chem. Soc., Faraday Trans. 1* **1986**, *82*, 767
(18) Sharma, V. K.; Wokaun, A.; Baiker, A. *J. Phys. Chem.* **1986**, *90*, 2715.
(19) Jhansi Lakshmi, L.; Narsimha, K.; Kanta Rao, P. *Appl. Catal., A* **1993**, *94*, 61.
(20) Eon, J. G.; Olier, R.; Volta, J. C. *J. Catal.* **1994**, *145*, 318.
(21) Roozeboom, F.; Fransen, T.; Mars, P.; Gellings, P. J. *Z. Anorg. Allg. Chem.* **1979**, *449*, 25.
(22) Wachs, I. E. *Catal. Today* **1996**, *27*, 437.
(23) Che, M.; Canosa, B.; Gonzalez-Elipe, A. R. *J. Phys. Chem.* **1986**, *90*, 618.
(24) Szakacs, S.; Altena, G. J.; Fransen, T.; Van Ommen, J. G.; Ross, J. R. H. *Catal. Today* **1993**, *16*, 237.
(25) Sohn, J. R.; Cho, S. G.; Pae, Y. I.; Hayashi, S. *J. Catal.* **1996**, *159*, 170.
(26) Occhiuzzi, M.; Tuti, S.; Cordischi, D.; Dragone, R.; Indovina, V. *J. Chem. Soc., Faraday Trans.* **1996**, *92*, 4337.
(27) Tanabe, K. *Mater. Chem. Phys.* **1985**, *13*, 347.
(28) Valigi, M.; Cimino, A.; Cordischi, D.; De Rossi, S.; Ferrari, C.; Ferraris, G.; Gazzoli, D.; Indovina, V.; Occhiuzzi, M. *Solid State Ionics* **1993**, *63−65*, 136.
(29) Zirconium in catalysis. Moles, P. J., Ed.; *Catal. Today* **1994**, *20*.
(30) Bosch, H.; Janssen, F. *Catal. Today* **1988**, *2*, 369.
(31) Indovina, V.; Occhiuzzi, M.; Ciambelli, P.; Sannino, D.; Ghiotti, G.; Prinetto, F. *Studies in Surface Science and Catalysis*; Hightower, J. W., Delgass, N. W., Iglesia, E., Bell, A. T., Eds.; Elsevier Science Publ., Amsterdam, 1996; Vol. 101, p 691.
(32) Cimino, A.; Cordischi, D.; De Rossi, S.; Ferraris, G.; Gazzoli, D.; Indovina, V.; Minelli, G.; Occhiuzzi, M.; Valigi, M. *J. Catal.* **1991**, *127*, 744−760, 761−776, 777−787.
(33) Sanati, M.; Andersson, A.; Wallenberg, L. R.; Rebenstorf, B. *Appl. Catal., A* **1993**, *106*, 51.
(34) Cimino, A.; Gazzoli, D.; Valigi, M *J. Electron Spectrosc. Relat. Phenom.* **1994**, *67*, 429.
(35) Busca, G.; Lorenzelli, V. *Mater. Chem. Phys.* **1982**, *7*, 89.
(36) Laane, J.; Ohlsen, J. R. *Prog. Inorg. Chem.* **1980**, *27*, 465.
(37) Pope, M. T. In *Heteropoly and isopoly oxometalates*; Springer-Verlag: Berlin, 1983; Chapter 3.
(38) Griffith, W. P.; Lesniak, P. J. B. *J. Chem. Soc.* A **1969**, 1066.
(39) Went, G. T.; Oyama, S. T.; Bell, A. T. *J. Phys. Chem.* **1990**, *94*, 4240.
(40) Tsyganenko, A. A.; Filimonov, V. N. *J. Mol. Struct.* **1973**, *19*, 579.
(41) Bensitel, M.; Saur, O.; Lavalley, J. C. *Mater. Chem. Phys.* **1987**, *17*, 249.
(42) Prinetto, F.; Cerrato, G.; Ghiotti, G.; Chiorino, A.; Campa, M. C.; Gazzoli, D.; Indovina, V. *J. Phys. Chem.* **1995**, *99*, 5556.
(43) Ghiotti, G.; Chiorino, A. *Spectrochim. Acta* **1993**, *49 A, N. 9*, 1345.
(44) Busca, G.; Lavalley, J. C. *Spectrochim Acta* **1986**, *42 A, N. 4*, 443.
(45) Busca, G. *Langmuir* **1986**, *2*, 577.
(46) Busca, G. *Mater. Chem. Phys.* **1988**, *19*, 157.
(47) Mori, K.; Miyamoto, A.; Murakami, Y. *J. Chem. Soc., Faraday Trans.* **1987**, *83*, 3303.
(48) Greenwood, N. N.; Earnshaw, A. *Chemistry of Elements*; Pergamon Press: U.K., 1993; p 279.
(49) Kim, D. S.; Segawa, K.; Soeya, T.; Wachs, I. E. *J. Catal.* **1991**, *136*, 744.